Title
Geochemical and tectonic uplift controls on rock nitrogen inputs across terrestrial ecosystems

Authors
Morford, Scott L
Houlton, Benjamin Z
Dahlgren, Randy A

RESEARCH ARTICLE

Key Points:
- Surficial sedimentary and metasedimentary rocks host large N reservoirs
- Lithology and tectonics strongly influence rock N erosion and input rates in terrestrial ecosystems
- Rock N fluxes can exceed atmospheric N inputs among denuding landscapes

Supporting Information:
- Data Set S1
- Figure S1 and Tables S1–S5

Correspondence to:
S. L. Morford,
slmorford@ucdavis.edu

Geochemical and tectonic uplift controls on rock nitrogen inputs across terrestrial ecosystems

Scott L. Morford[1], Benjamin Z. Houlton[1], and Randy A. Dahlgren[1]

[1]Department of Land, Air and Water Resources, University of California, Davis, California, USA

Abstract Rock contains $> 99\%$ of Earth's reactive nitrogen (N), but questions remain over the direct importance of rock N weathering inputs to terrestrial biogeochemical cycling. Here we investigate the factors that regulate rock N abundance and develop a new model for quantifying rock N mobilization fluxes across desert to temperate rainforest ecosystems in California, USA. We analyzed the N content of 968 rock samples from 531 locations and compiled 178 cosmogenically derived denudation estimates from across the region to identify landscapes and ecosystems where rocks account for a significant fraction of terrestrial N inputs. Strong coherence between rock N content and geophysical factors, such as protolith, (i.e. parent rock), grain size, and thermal history, are observed. A spatial model that combines rock geochemistry with lithology and topography demonstrates that average rock N reservoirs range from 0.18 to 1.2 kg N m^{-3} (80 to 534 mg N kg^{-1}) across the nine geomorphic provinces of California and estimates a rock N denudation flux of 20–92 Gg yr^{-1} across the entire study area (natural atmospheric inputs ~ 140 Gg yr^{-1}). The model highlights regional differences in rock N mobilization and points to the Coast Ranges, Transverse Ranges, and the Klamath Mountains as regions where rock N could contribute meaningfully to ecosystem N cycling. Contrasting these data to global compilations suggests that our findings are broadly applicable beyond California and that the N abundance and variability in rock are well constrained across most of the Earth system.

1. Introduction

Quantifying the magnitude and pattern of terrestrial nitrogen (N) inputs is crucial for predicting future carbon (C) uptake and storage in the terrestrial biosphere [*Hungate et al.*, 2003]. Past studies of N input fluxes in land ecosystems and their importance in regulating ecosystem structure and functioning have focused on primarily atmospheric sources of N [*Cleveland et al.*, 2013; *Vitousek and Howarth*, 1991; *Wang and Houlton*, 2009]. Crustal rock could contribute additional amounts of N to key ecosystem pools, however, given the widespread nature of N-rich parent materials and the massive size of this N reservoir in the Earth system (supporting information Table S1). Indeed, early biogeochemical studies pointed to the potential importance of bedrock N in global N budgets [*Hutchinson*, 1944; *Rayleigh*, 1939] and a number of recent studies have supported the idea that rocks are an overlooked source of N to terrestrial and aquatic ecosystems [*Cornwell and Stone*, 1968; *Dixon et al.*, 2012; *Hendry et al.*, 1984; *Holloway et al.*, 1998; *Montross et al.*, 2013; *Morford et al.*, 2011; *Strathouse et al.*, 1980]. However, incomplete knowledge of controls on the chemistry, denudation, and chemical weathering of rock N sources across terrestrial landscapes has limited our understanding of this N input pathway [e.g., *Ciais et al.*, 2013; *Houlton and Morford*, 2015]. Here we investigate rock N concentrations in combination with denudation rates across diverse spatial and geomorphic domains to better constrain the abundance of N reservoirs found in bedrock and the conditions under which rock N exhumation and denudation account for a significant fraction of ecosystem N balances.

Several factors could contribute to variations in rock N contents, thus affecting the magnitude of rock N weathering inputs to the terrestrial biosphere. Of particular importance is the initial N composition of rock materials and the lithification environment. Sedimentary, metasedimentary, and some hydrothermally altered rocks, for example, are derived from the burial of organic matter (OM) in marine, lacustrine, and fluvial sediments where diagenesis and subsequent metamorphism preserve N in organic and mineral forms [*Boyd*, 2001]. Nitrogen from the mantle is also incorporated into some igneous rocks, such as basalt [*Marty*, 1995] but at lower concentrations than are typically found in rocks of sedimentary origin [*Holloway and Dahlgren*, 2002]. These differences between the origin of rocks and their histories give rise to several orders of magnitude variation in the N content of parent materials that underlie terrestrial ecosystems.

Further, the N content of sedimentary and metasedimentary rocks is intimately coupled to the lithification of organic C in sediments [*Hedges and Keil*, 1995; *Muller*, 1977] and varies as a function of the burial efficiency of

organic matter in sediments, as well as the thermal environment during diagenesis and metamorphism. Fine-grained siliciclastic sedimentary rocks such as shale and mudstone typically have higher N concentrations than their coarse-grained counterparts (e.g., sandstones and conglomerate) due to the protection of OM on minerals with highly reactive surface areas [*Kennedy et al.*, 2002]. These general trends are further modulated by oxygen dynamics of the sediments during burial, as oxidative degradation of OM is attenuated in anoxic basins and at continental margins where sediment accumulation is rapid [*Hartnett et al.*, 1998].

After burial, the thermal environment and mineralogy of the sediments play an additional role in controlling the retention and form of N in rock. Sedimentary and metasedimentary rocks contain both organic and mineral forms of N [*Miller*, 1903; *Stevenson*, 1959], but progressive heating during burial diagenesis and metamorphism results in thermal mineralization of organic N to ammonium (NH_4^+) [*Boudou et al.*, 2008]. The mineral N can be incorporated into silicate minerals or lost from the rock via hydrothermal fluid flow or volatilization reactions [*Bebout and Fogel*, 1992]. The total N content of the source rock may decline during progressive heating as a function of the abundance of compatible minerals (e.g., micas and feldspars) resulting in high-grade metamorphic rocks generally containing substantially less N than the sediments from which they were derived.

In addition to controls on rock N chemistry, tectonics and climate interactively control the rate of rock exhumation and chemical weathering across the terrestrial surface [*Gaillardet et al.*, 1999; *Kump et al.*, 2000; *Stallard and Edmond*, 1983]. Denudation rates in particular are strongly correlated with chemical fluxes from regolith and soil [*Riebe et al.*, 2004], suggesting that rock N mobilization and weathering fluxes will be highest among moderate to rapidly denuding landscapes. Chemical weathering rates likely differ between organic and silicate mineral N reservoirs in rocks [*Bolton et al.*, 2006; *Petsch et al.*, 2000], as the former is more susceptible to rapid oxidative weathering and may not be as sensitive to kinetic limitation of acid hydrolysis reactions, particularly among highly erosive landscapes [*Calmels et al.*, 2007; *Hilton et al.*, 2014; *West et al.*, 2005]. Together, these factors suggest that spatial patterns of rock N mobilization in terrestrial ecosystems are governed interactively by geochemistry and tectonics, and the fraction of rock N that is chemically weathered is further constrained by climate and the composition of the N reservoir (i.e., organic versus silicate N).

We evaluated trends of N concentration across different rock types from a large and diverse geographic area and investigated how interactions on rock geochemistry, lithology, and tectonics regulate the rock N denudation flux. Importantly, our analysis does not directly consider the influence of climate and hydrologic factors on rock N denudation and weathering. These factors, particularly through controlling runoff and stream power, play an important role in regulating mass fluxes from bedrock at basin scales [*Howard et al.*, 1994; *Kump et al.*, 2000; *Maher and Chamberlain*, 2014] but are difficult to integrate into predictive models over large spatial domains. Rather, our analysis emphasizes the role of topographic relief in regulating the N denudation flux, which is strongly correlated with denudation rates across the terrestrial system [*Montgomery and Brandon*, 2002; *Portenga and Bierman*, 2011; *Summerfield and Hulton*, 1994].

Our analysis addresses two related hypotheses. First, rock N reservoirs are coherent across landscapes and can be estimated with some knowledge of rock types and geologic histories. Second, patterns of N denudation across landscapes reflect the combined influence of tectonics and lithology N concentration, rather than N concentration alone. To test our hypotheses, we examined rock N content in combination with denudation using a spatial framework. Our approach combined N lithology and denudation models to estimate the rock N flux across differing geomorphic regions and ecosystem types. We parameterized the N lithology model using 968 rock samples collected across California, and N denudation rates were modeled using 178 catchment scale [10]Be measurements compiled from California watersheds. Our combined model is the first to estimate a large-scale rock N flux—and places an upper bound constraint on the rock N chemical flux to ecosystems of California.

2. Methods

2.1. Sample Collection and Preparation

We sampled 968 different rocks from 531 locations across the Pacific Coast of the U.S. (i.e., southern Oregon to southern California, Figure 7). Regional geologic maps (1:250000 scale) from the California Geological Survey were used to identify time stratigraphic units, and a stratified sampling regime was used to maximize collection of sedimentary and metasedimentary lithologies across a lithology-by-age matrix. Minimally

Table 1. Rock Nitrogen Concentration in the 968 Samples Analyzed in This Study[a]

	Total Nitrogen (mg kg^{-1})								Probability Distribution	
	Q0	Q10	Q25	Q50	Q75	Q90	Q100	n	Skewness	Kurtosis (β_2)
Fine-grained siliciclastic[b]	<20	278	453	698	907	1242	7154	537	3.95	26.25
Coarse-grained siliciclastic[c]	57	144	202	271	376	523	3680	217	5.84	44.95
Carbonates[d]	45	134	156	307	461	1128	1910	53	1.82	5.86
Siliceous[e]	53	75	111	157	201	287	1792	24	3.11	13.16
Igneous[f]	<20	<20	55	80	130	183	280	94	0.97	3.67
High-grade metamorphic[g]	41	81	99	148	232	305	35390	40	3.58	18.34

[a]Percentile data are presented to illustrate the range of values observed across different rock types: lowest (0th percentile—Q0) to highest values (100th percentile—Q100); Q50 corresponds to median value.
[b]Fine-grained siliciclastic rocks and their low-grade metamorphic counterparts including argillite, mudstones, siltstone, shale, slate, phyllite, and mica schist.
[c]Coarse-grained siliciclastic rocks and their low-grade metamorphic counterparts including sandstone, conglomerate, greywacke, and quartzite.
[d]Carbonates and metacarbonates: limestone, dolomite, and marble.
[e]Silicic rocks: chert and metachert.
[f]Igneous rocks: granite, diorite, gabbro, rhyolite, andesite, and basalt.
[g]High-grade metamorphic rocks (distinguished from low-grade metamorphic rocks by lack of chlorite minerals): gneiss, amphibolite, upper greenschist facies (no chlorite), hornfels, granulites, and hydrothermally altered igneous rocks. The distinction between high-grade and low-grade metamorphisms is based upon the recognition that N devolatilizes from rocks at temperatures above ~450°, corresponding with dehydration of mica and chlorite minerals [*Bebout and Fogel*, 1992].

weathered bedrock was sampled from fresh road cuts or intact outcrops. At locations where multiple rock units were observable, we collected up to three independent samples to characterize the variability among lithologies. Rock samples were sorted into one of six lithological categories based on field and laboratory determination of rock type, protolith, and metamorphic grade (Table 1). In cases where classification of metamorphic rocks was not achievable using hand samples or field geologic data, samples were identified using geochemical data and/or thin-section microscopy.

2.2. Rock Analysis

In the laboratory, any rock weathering rind was removed using a lapidary slab saw. Unweathered subsamples were treated with 5% hydrogen peroxide for 24 h at room temperature (22 ± 1°C) to remove surficial organic contaminants and then heated to 100°C to decompose the hydrogen peroxide. Samples were dried and crushed with a hydraulic press to particle sizes < 10 mm in diameter. Next, samples were washed with deionized water and dried at 110°C for 48 h. A 60 g subsample was pulverized using a hardened-steel shatter box to pass a standard U.S. 200 mesh (74 μm) sieve.

Rock pretreatment procedures were compared to a potassium hypobromite (KOBr) digestion procedure [*Silva and Bremner*, 1966] to determine if oxidation, washing, and grinding resulted in rock N loss prior to
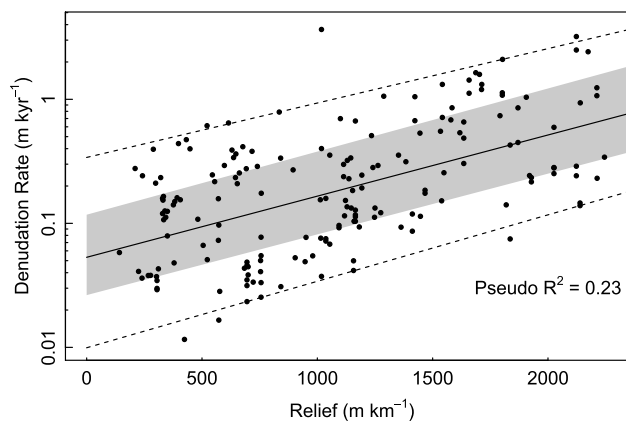
**Figure 1.** Model fit for denudation data using quantile regression model (equation (1)). Solid line represents the median model estimate ($\tau = 0.5$) and shaded area bound the 25th to 75th quantiles ($\tau = 0.25$–0.75). Dashed lines represent the 95% prediction interval ($\tau = 0.025$–0.975). Pseudo R^2 of the median model ($\tau = 0.5$) using methodology from *Koenker and Machado* [1999].
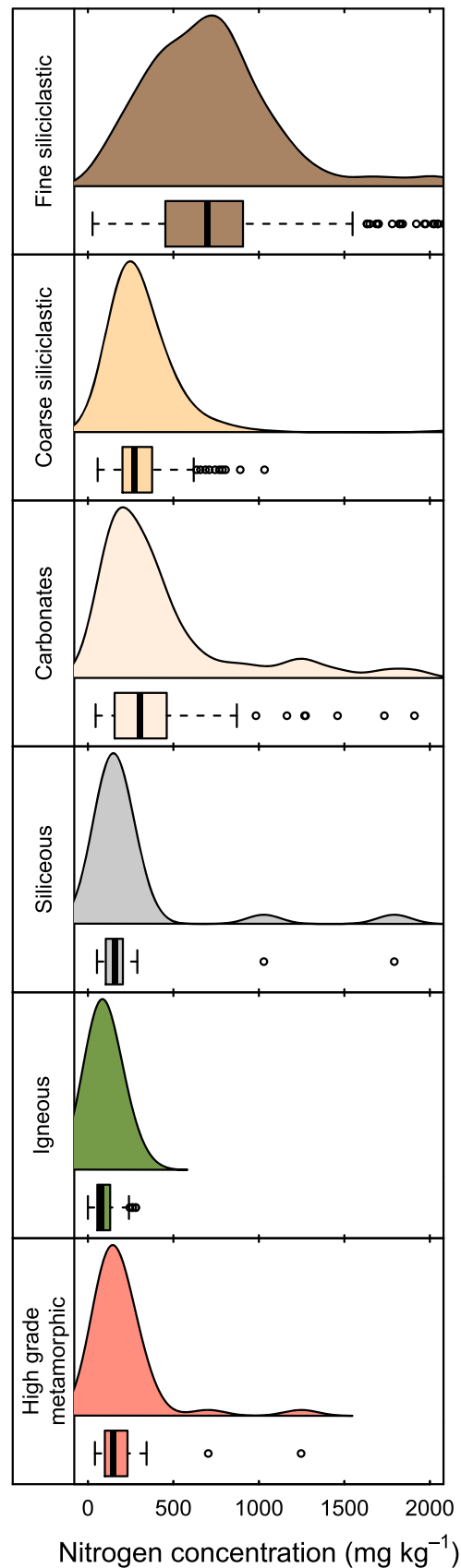
analysis. The KOBr removes modern organic N and exchangeable N from mineral samples but does not remove rock-derived N (mineral and organic). We found less than a 6% difference in rock N values between samples treated by our rock pretreatment procedures and the KOBr digestion for rocks hosting both mineral and organic N reservoirs (supporting information Table S2), suggesting that the two methods provide similar results when preparing samples. Our method was not quantitative for vesicle N gas that can be found in some volcanic rocks and glasses; however, these rock N reservoirs do not contribute substantially to rock N abundance on a mass basis [*Javoy and Pineau*, 1991]. Additionally, our method was not quantitative for nitrate and ammonium salts that may have accumulated in rock samples due to long-term atmospheric N deposition.

We used an Elementar Vario EL cube elemental analyzer with a combustion temperature of 1800°C (1050°C oven temperature) to quantify total N and C and a PDZ Europa 20-20 isotope ratio mass spectrometer (Sercon Ltd., Cheshire, UK) to quantify $^{13}C/^{12}C$. The detection limit for our samples was $20\,\mu g\,N$ and $100\,\mu g\,C$ (100 mg sample size); rock replicates ($n = 135$) had an average relative standard deviation (RSD) for N of 11.2% for rocks $<200\,mg\,N\,kg^{-1}$ and 3.2% for rocks $>200\,mg\,N\,kg^{-1}$. The RSD for total C was 2.4%, and the $^{13}C/^{12}C$ standard deviation was <0.2‰. Measurements ($n = 33$) of the B2152 sediment standard (Elemental MicroAnalysis, Devon U.K.) averaged $1071 \pm 17\,mg\,N\,kg^{-1}$ (accepted $= 1020 \pm 100\,mg\,N\,kg^{-1}$) and $1.27 \pm 0.02\%$ C (accepted $= 1.27 \pm 0.1\%$ C). We assume that total C equals organic C where sample $^{13}C/^{12}C < -20$‰ [*Hoefs*, 2009]. Total aluminum (Al) and potassium (K) were determined on a subset of samples by inductively coupled plasma optical emission spectrometry (ICP-OES) following lithium metaborate fusion (AcmeLabs, Vancouver, BC) with RSDs $< 2\%$. ICP-OES data quality was assessed by analysis of blind standards (U.S. Geological Survey BCR-2 (Basalt, Columbia River)) and sample duplicates (supporting information

Figure 2. Total nitrogen concentration across all 968 geologic samples. Samples are separated into six categories based upon protolith and postdepositional processes. A kernel density function and boxplot are presented for each group to characterize the distribution of values. The data show substantial N enrichment in fine-grained siliciclastic rocks. Rock N reservoirs on a mass:volume ratio presented in supporting information Figure S1.
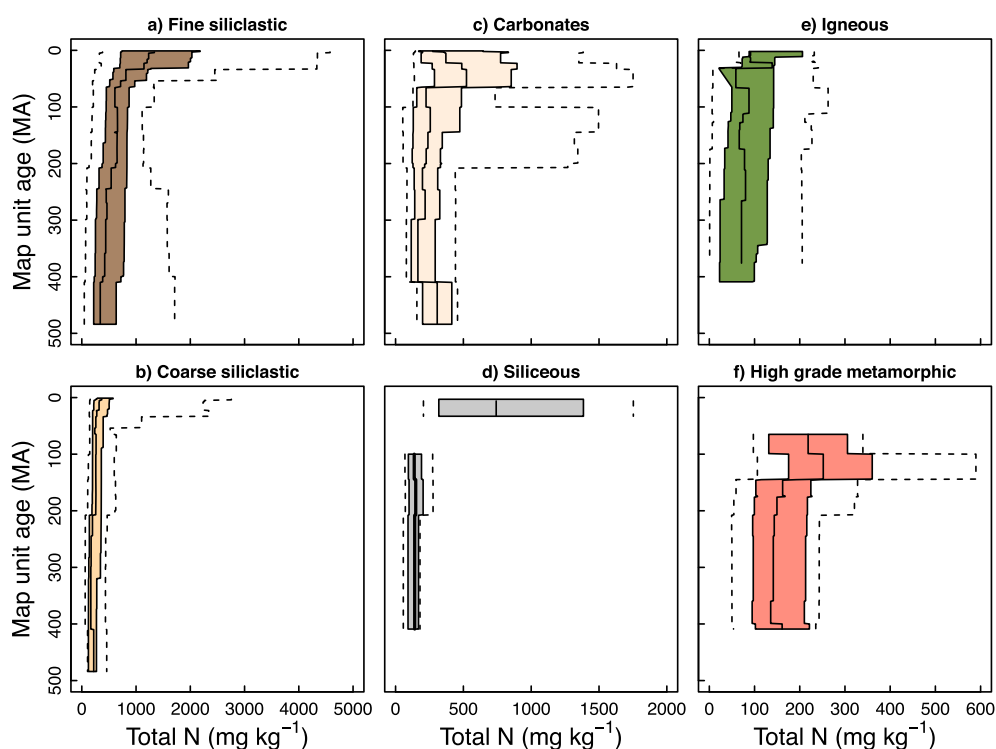
Figure 3. Nitrogen concentration as a function of rock type and geologic age. Colored regions span 25th–75th percentile and dashed lines bound the 95% confidence interval; note that the *x* axis differs for each column.

Table S3). Of the 22 BCR-2 standard comparisons, 21 were within 1 standard deviation of the accepted value, with an average relative percent difference (RPD) of 1.3% (range: 0.0–5.8%) between accepted and measured values. Across all duplicates, the average specific RPD was 1.2% (range: 0.0–5.8%).

Statistical comparisons among rock types and rock ages were performed pairwise using the nonparametric Mann–Whitney *U* test in R [*R Core Team*, 2014]. A total of 26 pairwise comparisons were performed.

2.3. Lithology Model

We modeled the spatial distribution of surficial rock N reservoirs (representing the upper ~5 m of bedrock) across California using geochemistry and lithology data from our sample set, sample age estimates extracted from 1:250,000 regional geology maps, map units derived at a 1:750,000 scale [*Ludington et al.*, 2005], and rock density data derived from the literature (supporting information Table S4). First, we developed a lithology-by-age model from our data by applying a slice-wise aggregation algorithm [*Beaudette et al.*, 2013] to estimate median and quantile values for each lithology group as a function of geologic age. Next, we applied these median rock N concentrations to mapping units based on bedrock age and lithology type. In cases where multiple lithologies were identified within a given grid cell (i.e., shale + sandstone), we assumed that each identified rock type contributed an equal fraction. This approach is conservative in terms of estimating rock N concentrations; fine-grained sediments are typically dominant across siliciclastic map units in North America [*Suchet et al.*, 2003] and are enriched in N relative to their coarse-grained counterparts (see results). Franciscan mélange (mixed heterogeneous lithologies derived from subduction zones) map units were assigned rock N values of 456 mg kg^{-1}, corresponding to the median rock N value (range = 45–1230 mg kg^{-1}) of the 68 samples taken within those map units. To estimate rock N concentrations of quaternary alluvium mapping units, we performed watershed segmentation and identified the contributing area of sediment from upland positions. Mean area-weighted rock N concentrations were then calculated for the upland component of each watershed basin and applied to the alluvial map unit. This segmentation approach does not consider weathering of rock N reservoirs prior to redeposition in unconsolidated alluvial sediments and thus may overestimate N contents within these environments, particularly
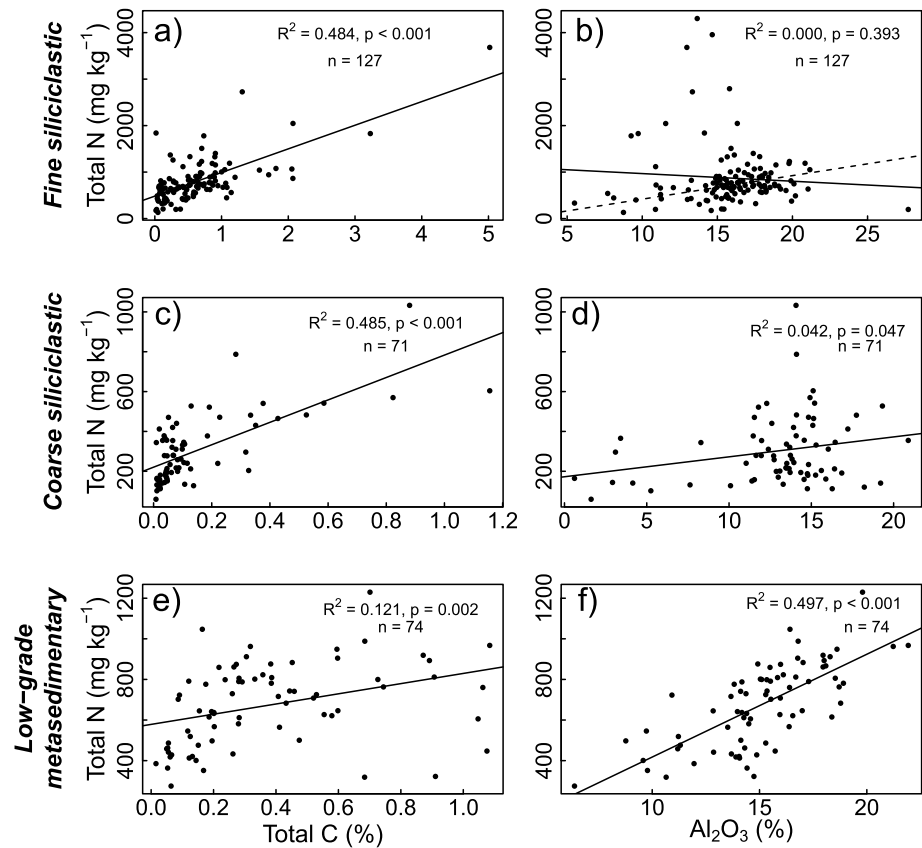
Figure 4. (a, c, and e) Total nitrogen versus organic carbon and (b, d, and f) total nitrogen versus aluminum for fine- and coarse-grained siliciclastic rock samples. Metasedimentary rocks have been separated from their sedimentary counterparts to illustrate differences in rock N reservoirs as a function of postdepositional processing. The regression derived in Figure 4f is plotted in Figure 4b (dashed line). To remove the potential influence of carbonates, only samples with bulk $\delta^{13}C < -20$‰ were used in the model.

where lowland sediments are fed by upland environments with a high degree of chemical weathering. Finally, we multiplied rock N concentrations by corresponding rock density data (supporting information Table S4) within each mapping unit, with density estimates ranging from $2000\,kg\,m^{-3}$ for alluvium to $2950\,kg\,m^{-3}$ for basalt; density of mélange units was estimated to be $2400\,kg\,m^{-3}$.

2.4. Denudation Model

We utilized long-term, catchment-scale ^{10}Be cosmogenic radionuclide measurements in California watersheds ($n = 178$) to estimate landscape denudation rates [*Balco et al.*, 2013; *Gudmundsdottir et al.*, 2013; *Portenga and Bierman*, 2011]. We regressed denudation rates against mean local relief derived from 30 m Shuttle Radar Topography Mission topography [*U.S. Geological Survey*, 2004], as denudation is correlated with topographic relief and slope at large spatial scales [*Montgomery and Brandon*, 2002; *Portenga and Bierman*, 2011]. Local relief was calculated as the difference between maximum and minimum elevation within a radius of 5 km at each grid cell (Albers Equal Area Conic projection) using the r.neighbors function in a geographic information system (GIS) [*GRASS Development Team*, 2012]. We used a nonparametric quantile regression model [*Koenker*, 2013] to evaluate the dependency of denudation on topographic relief in R [*R Core Team*, 2014]. The functional form of our denudation model reflects the exponential relationship between denudation and topography [*Montgomery and Brandon*, 2002; *Willenbring et al.*, 2013]:

$$Q_D(\tau|\text{relief}) = \beta_0(\tau) + \beta_{\text{relief}}(\tau)\exp(\text{relief}) \qquad (1)$$

where denudation (Q_D, units: length time^{-1}) increases exponentially with *relief* (Figure 1). Denudation rates were calculated at the 0th, 2.5th, 10th, 25th, 50th, 75th, 90th, and 97.5th quantiles (τ) to provide a probability
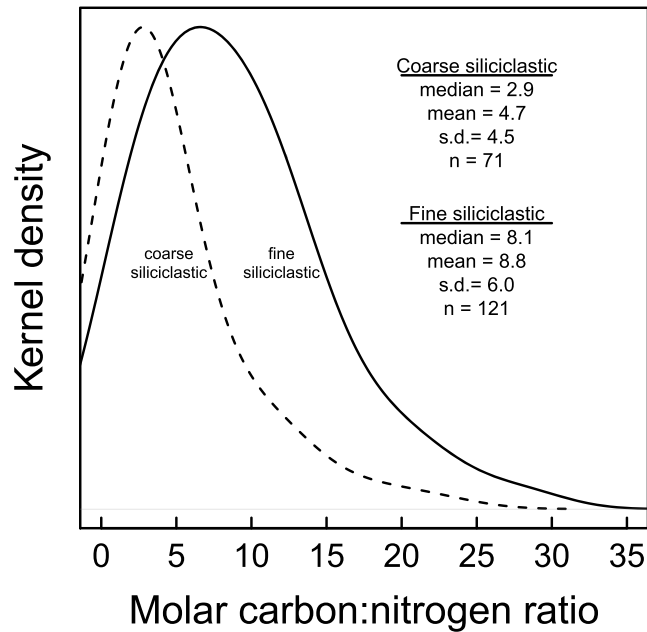
Figure 5. Carbon:nitrogen ratio (mol:mol) of fine-grained siliciclastic (solid line) and coarse-grained siliciclastic (dashed line) sedimentary rocks. Calcareous siliciclastic rocks excluded from compilation.

distribution rather than a single, mean-field estimate. Nitrogen denudation ($D_{N,\tau}$, units: mass area^{-1} time^{-1}) rates were then calculated at each grid cell using N concentration data from our model $[N]_{rock}$:

$$D_{N,\tau} = Q_{D,\tau} \cdot \rho \cdot [N]_{rock} \cdot A \qquad (2)$$

where A is grid cell area and ρ is rock density. Denudation rates were evaluated among nine geomorphic provinces [*California Geological Survey*, 2002] in California to investigate how dominant landforms and rock types contributed to rock N input fluxes. To simplify our analysis, the Modoc plateau was joined with the Cascades, and the Colorado Desert was joined with the Mojave Desert. The gridded data were segmented in GIS and then analyzed in R to compute quantiles, interquartile range, and empirical cumulative distribution functions of the segmented regions.

Application of CRN derived denudation rates to predict the rock N denudation flux has limitations. CRN denudation measurements are biased toward coarse-grained lithologies, such as felsic igneous rocks and sandstones, and may not accurately represent denudation rates among fine-grained sedimentary rocks due to
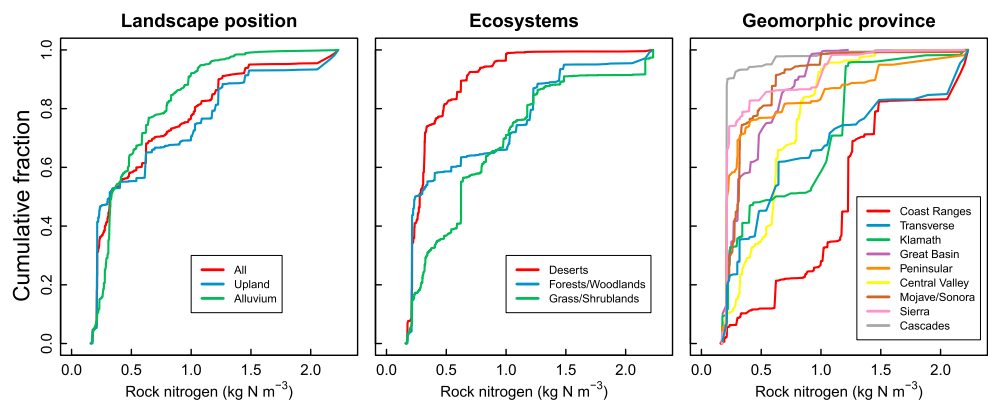
Figure 6. Cumulative probability for rock nitrogen content across (left) landscape position, (middle) ecosystem type, and (right) geomorphic province from our lithology model. Map of geomorphic provinces provided in Figure 10.
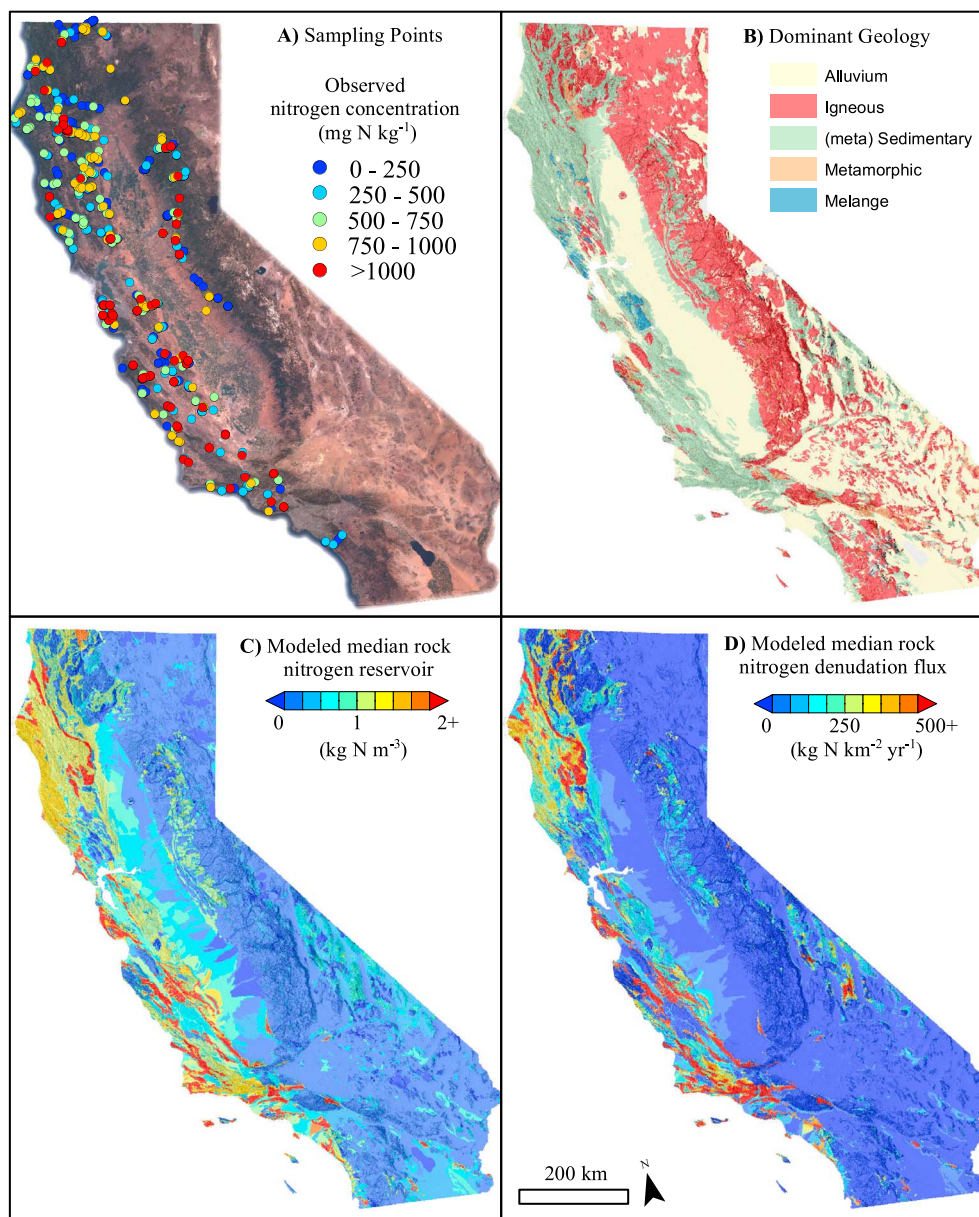
Figure 7. Rock nitrogen reservoirs and mobilization. (a) Sampling locations and measured rock N. Point data reflect the highest N concentration observed at a particular sampling site when multiple samples were taken. (b) Dominant geologic units. (c) Modeled median N reservoirs in rock. (d) Modeled median N denudation flux illustrating the mobilization potential for rock N across the study area.

their lack of recoverable quartz. Additionally, our model does not incorporate factors such as rock strength, land sliding, and land use change that can contribute to higher short-term denudation rates than the long-term CRN denudation values would suggest. We address these limitations in our discussion below.

3. Results

3.1. Nitrogen Reservoirs and Geochemistry

Our analysis of total N showed that among the six rock categories, four significantly different ($p < 0.005$, nonparametric pairwise comparisons) rock groups emerged: fine-grained siliciclastic rocks > coarse-grained siliciclastic and carbonate rocks > siliceous and high-grade metamorphic > igneous. The median total N content of all rocks
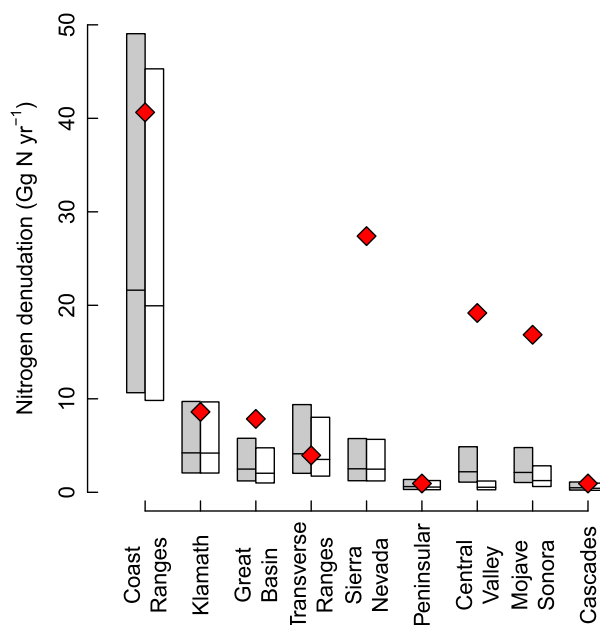
Figure 8. Rock nitrogen denudation estimates by geomorphic province. Estimates span the 25th–75th quantiles in our denudation regression model. Gray boxes include total area, while white boxes include only upland (nonalluvial) landscapes. Estimates of natural atmospheric N inputs (biological fixation + deposition) presented as red diamonds for comparison. Map of geomorphic provinces provided in Figure 10.

sampled was 426 mg kg^{-1} ($n = 968$) with coherent variation both among and within rock types. Fine-grained siliciclastic rocks had the highest median N content (698 mg kg^{-1}), while igneous rocks contained the lowest (80 mg N kg^{-1}, Figure 2 and Table 1). Coarse-grained siliciclastic rocks and carbonate rocks contained intermediate N concentrations (median N of 271 and 307 mg kg^{-1}, respectively), while siliceous (157 mg kg^{-1}) and high-grade metamorphic rocks (148 mg kg^{-1}) contained substantially less N. Distributions for all groups exhibited nonnormal, positive skew, with the exception of igneous rocks.

Nitrogen content also varied by geologic age for sedimentary lithologies; younger rocks contained more N than older rocks (Figure 3). Median N concentrations were higher in Cenozoic fine-grained siliciclastic rocks (972 mg kg^{-1}, $n = 134$) versus Mesozoic (648 mg kg^{-1}, $n = 316$, $p < 0.001$) and Paleozoic (422 mg kg^{-1}, $n = 68$, $p < 0.001$) counterparts. Median N content of Cenozoic carbonate rocks (median = 488 mg kg^{-1}, $n = 32$) was found to be more than double its older Mesozoic (226 mg kg^{-1}, $n = 21$, $p = 0.04$) and Paleozoic (221 mg kg^{-1}, $n = 8$, $p = 0.02$) counterparts. Median N values for Cenozoic siliceous rocks (656 mg kg^{-1}, $n = 5$) exceeded older rocks by more than a factor of 3 (Mesozoic: 136 mg kg^{-1}, $n = 19$, $p = 0.006$; Paleozoic: 149 mg kg^{-1}, $n = 4$, $p = 0.02$). In coarse-grained siliciclastic rocks, Cenozoic (271 mg kg^{-1}, $n = 95$) and Mesozoic (258 mg kg^{-1}, $n = 120$, $p = 0.03$) rocks have similar median N concentrations but were higher than Paleozoic rocks (171 mg kg^{-1}, $n = 20$, $p < 0.001$). In contrast, igneous rocks contained similar N concentrations across all age classes (median: 75–83 mg kg^{-1}, $n = 93$, $p > 0.73$). High-grade metamorphic rocks showed similar median N concentrations between Mesozoic (171 mg kg^{-1}, $n = 19$) and Paleozoic eras (148 mg kg^{-1}, $n = 20$, $p = 0.52$), but Cretaceous rocks contained more N on average (median = 259, $n = 10$, $p = 0.02$) than other Mesozoic rocks. However, differences in N content among high-grade metamorphic rocks may be driven in part by differences in protolith (i.e., parent rock), which were not assessed.
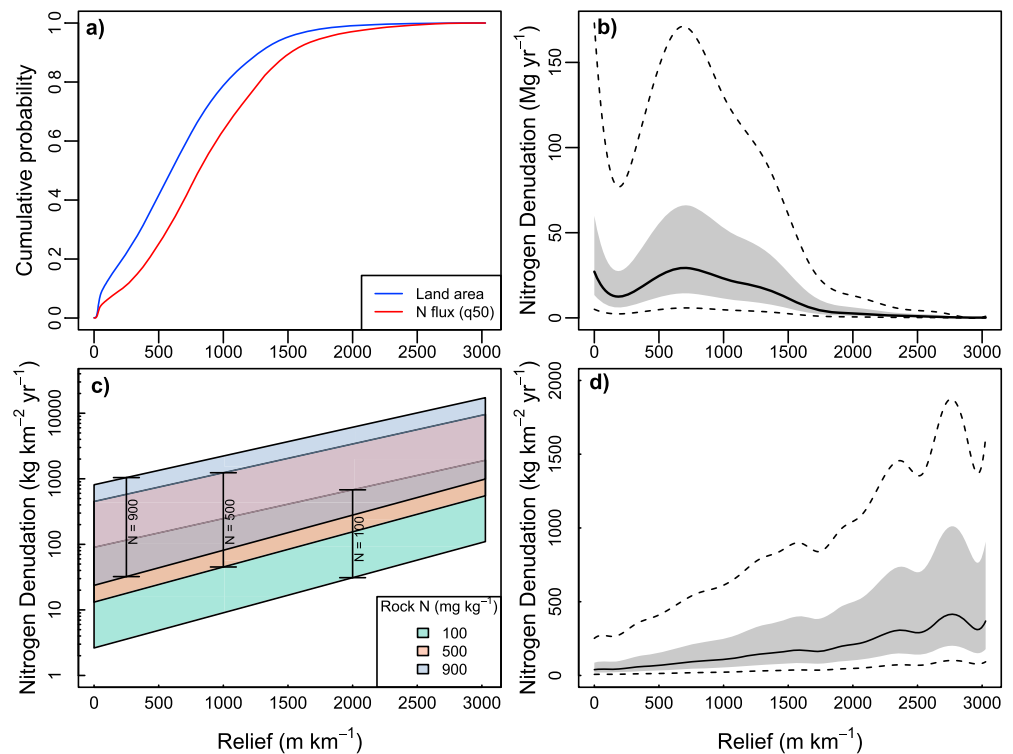
The N content of siliciclastic rocks was positively correlated with C and Al in sedimentary and metasedimentary classes, respectively (Figure 4). Total (organic) C explained roughly half of the variation in the N content of coarse-grained ($R^2 = 0.485$) and fine-grained ($R^2 = 0.484$) sedimentary siliciclastic rocks. However, in metasediments the correlation with C was much weaker ($R^2 = 0.121$) and N was more strongly correlated with Al content ($R^2 = 0.497$). No significant relationship between Al and N was found in coarse-grained ($R^2 = 0.024$) or fine-grained ($R^2 < 0.001$) siliciclastic sedimentary samples. Median C:N ratios (molar) for coarse- and fine-grained siliciclastic sedimentary rocks were 2.9 and 8.1, respectively (Figure 5).

3.2. Nitrogen Lithology Model

The median surficial N concentration across all of California was estimated to be 159 mg N kg^{-1} but estimates varied substantially among geomorphic provinces as a function of differing rock types and ages (median range: 80–534 mg N kg^{-1}, supporting information Table S5). The highest median lithology N concentration is found in the sedimentary rock dominated Coast Ranges (534 mg N kg^{-1}), while igneous provinces of the Sierra Nevada, Cascades, and Peninsular Ranges had the lowest median lithology N concentrations (80 mg N kg^{-1}).
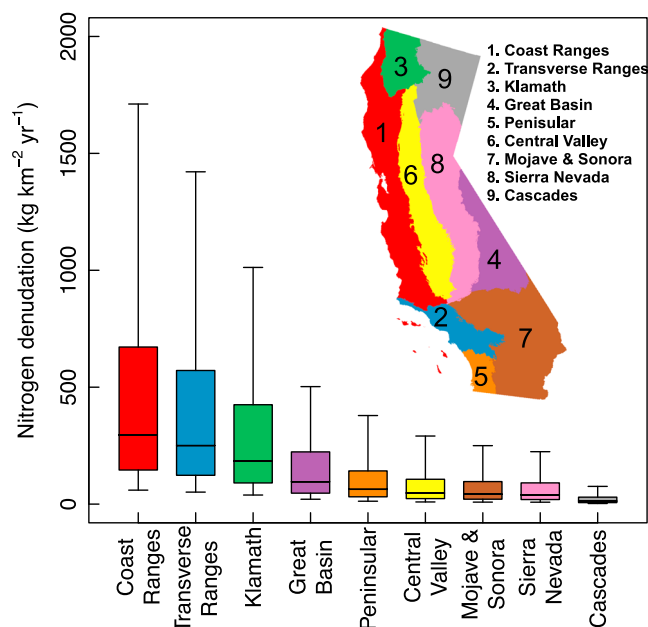
Figure 9. Modeled nitrogen denudation rates across our study area. (a) Empirical distribution function for median nitrogen denudation flux (red) and contributing area (blue). (b) Modeled total nitrogen denudation as a function of landscape relief. Shaded area represents 25th and 75th prediction interval; dashed lines encompass the 95% prediction interval. (c) 95% prediction interval for nitrogen denudation as a function of rock nitrogen concentration and landscape relief. (d) Area-averaged nitrogen denudation flux as a function of landscape relief. Shaded area represents 25th and 75th prediction interval; dashed lines encompass the 95% prediction interval.

Accounting for differences in rock density among lithologies, the model estimated a median surficial rock N reservoir of $0.33 \, kg \, N \, m^{-3}$ across the entire state. Median estimates for alluvial and upland positions were similar (0.32 and $0.34 \, kg \, N \, m^{-3}$, respectively), but upland positions showed a higher right skew (Figure 6). Rock N reservoirs varied substantially among geomorphic provinces (Figure 7c), with the Coast Ranges ($1.2 \, kg \, N \, m^{-3}$) hosting the largest reservoirs and the Cascades and Sierra Nevada hosting the lowest (0.18 and $0.21 \, kg \, N \, m^{-3}$, respectively).

3.3. Nitrogen Denudation Model

Nitrogen denudation simulations for California ecosystems predict a mobilization flux of $20–92 \, Gg \, N \, yr^{-1}$ statewide (*25th–75th percentile estimate*, median = $40 \, Gg \, yr^{-1}$). Denudation from alluvial systems accounted for 13% of the total N flux; considering only upland landscape positions developing on bedrock, our estimates ranged from 17 to $80 \, Gg \, N \, yr^{-1}$ (median = $35 \, Gg \, N \, yr^{-1}$). We observed substantial differences in N denudation rates among geomorphic provinces owing primarily to differences in dominant lithology and landscape relief (Figure 8). In our model, 32% of the land area accounted for half of the total N denudation flux, but the majority of the total N denudation flux was derived from landscapes with moderate mean local relief ($500–1500 \, m \, km^{-1}$, Figure 9). Forested landscapes account for 50% of the N denudation flux in the model, but only occupy 35% of the total land area.

The Coast Ranges accounted for 53% of the total N denudation flux across the study area, with a median N denudation rate of $3.2 \, kg \, ha^{-1} \, yr^{-1}$ (Figure 10). Considering the N denudation flux on an area-averaged basis, large denudation fluxes were observed among geomorphic provinces with moderate-to-high relief in combination with abundant sedimentary and metasedimentary lithologies (Coast Ranges, Transverse Ranges, and Klamath Mountains). Median N denudation fluxes in these provinces were more than double the flux estimated in provinces dominated by low-relief terrains (irrespective of rock N content) or provinces that have low rock N concentrations and moderate-to-high relief (Figure 10).

Figure 10. Boxplots showing modeled nitrogen denudation flux as function of geomorphic province. Flux estimates from upland areas only. Locations of the geomorphic provinces provided in the inset.

4. Discussion

4.1. Geophysical Controls on Rock Nitrogen Content

Our analysis reveals widespread distribution of N-rich rocks in many different kinds of terrestrial ecosystems and confirms our first hypothesis that rock N reservoirs are spatially coherent across different rock types. Specifically, $> 35\%$ of our 531 sampling sites had one or more rock samples that exceeded $500\,mg\,N\,kg^{-1}$, and of the sampling sites that had fine-grained siliciclastic rocks, 64% had one or more rock samples that exceeded $500\,mg\,N\,kg^{-1}$. These data suggest that soils developing from sedimentary parent materials contain substantial amounts of native, reactive N that could be chemically weathered similar to other rock-derived nutrients, such as phosphorus and calcium.

We also found important differences in N content within rock categories as a function of geologic age, supporting our hypothesis that geologic histories have important leverage on rock N concentrations. These differences are likely not directly attributable to the age of the rock but rather differences in depositional or postdepositional processes that control the accumulation and devolatilization of N from sediments during diagenesis and metamorphism. The differences in total N concentrations for sedimentary rocks of Mesozoic versus Cenozoic age in the Coast Ranges of California may reflect differences in thermal histories. Nitrogen is progressively mobilized (lost) from sediments during prograde diagenesis and metamorphism [*Bebout and Fogel*, 1992; *Bebout et al.*, 1999; *Williams et al.*, 1992], so it is not surprising that Coast Range Mesozoic sediments maturing in a subduction zone with temperatures exceeding 300°C are depleted in N relative to Cenozoic sedimentary rocks that have only undergone burial diagenesis (50–150°C) [*Compton et al.*, 1992; *Sadofsky and Bebout*, 2003].

Knowledge of the thermal alteration of sedimentary and metasedimentary rocks can be useful when assessing potential N enrichment of rocks with differing geologic histories. Thermal mineralization of organic N is initiated at temperatures of 80–140°C, corresponding with hydrocarbon mobilization [*Williams et al.*, 1992]. While not all N is released from organic reservoirs at these temperatures [*Boudou et al.*, 2008], substantial amounts of N are freed as NH_4^+ which can be fixed in silicate minerals or mobilized in pore fluids. Nitrogen is relatively stable in silicate minerals at low to moderate metamorphic temperatures where it behaves like large ion lithophiles (e.g., K^+, Rb^+, and Cs^+) [*Busigny et al.*, 2003] but is progressively lost from rock at temperatures > 300–500°C [*Bebout and Fogel*, 1992; *Pitcairn et al.*, 2005; *Williams and Ferrell*, 1991]. Temperature alteration of rock can be inferred from mineralogy and vitrinite reflectance, and N devolatilization from silicates is generally correlated with the dehydration (loss) of chlorite and/or muscovite in metasedimentary rocks.

Conceptually, this thermal framework suggests that sedimentary and metasedimentary siliciclastic rocks can be roughly segmented into three groups based upon the stability of N in organic and silicate reservoirs under differing temperature regimes. First, rock N concentrations are greatest in organic-rich rocks that have experienced shallow burial diagenesis ($<80°C$). Nitrogen concentrations in these rocks can exceed $2000\,mg\,N\,kg^{-1}$, with N primarily associated with C in organic matter. Second, sedimentary rocks from greater burial depths ($T > 80°C$) and low-grade metasedimentary rocks contain N reservoirs $< 2000\,mg\,kg^{-1}$, with N increasingly found as NH_4^+ in minerals as recalcitrant organic N pools are thermally decomposed under prograde diagenesis/metamorphism [*Boudou et al.*, 2008; *Busigny and Bebout*, 2013]. Finally, at metamorphic temperatures $> \sim450°C$, N reservoirs in rock are reduced further as NH_4^+ stabilized in hydrous minerals (e.g., mica) is largely devolatilized. Some N is retained during moderate temperature metamorphism in high-temperature micas and feldspars, but the maximum N concentration in these rocks is typically $< 400\,mg\,kg^{-1}$ [*Bebout and Fogel*, 1992; *Bebout et al.*, 1999].

4.2. Organic and Aluminosilicate N Reservoirs in Siliciclastic Rocks

The partitioning of N between organic and mineral forms in rock is important, because these reservoirs likely undergo different rates of chemical weathering. Rocks enriched in organic matter are more susceptible to rapid oxidative weathering processes versus those with low organic contents. Our geochemical data suggest that both organic and mineral N are present in siliciclastic sedimentary rocks. We observe a strong correlation between C and N abundance in these rocks, suggesting that much of the N is associated with sedimentary organic matter, particularly among rocks with high N content (Figure 4). However, two lines of evidence suggest that mineral N forms are also an important component of these reservoirs.

First, for fine- and coarse-grained siliciclastic rocks, the regression models between C and N had highly significant ($p < 0.001$) nonzero intercepts (482 and $220\,mg\,N\,kg^{-1}$, respectively) suggesting that these rocks contain N even in the absence of C. Further, a subset of fine-grained siliciclastic rocks did show a clustering around the Al:N regression line derived for metasedimentary rocks (Figure 4b, dashed line), suggesting that both organic and mineral N reservoirs are present in fine-grained sedimentary rocks and that aluminosilicate abundance plays a subordinate control on N retention in rocks of low-to-moderate N contents. These results are consistent with data from petroleum basins that suggest that inorganic N comprises between 30 and 70% of the total rock N reservoir [*Compton et al.*, 1992; *Jurisch et al.*, 2012; *Williams and Ferrell*, 1991].

Our data reveal strong correlations between rock N concentrations and Al in low-grade metasedimentary rocks, reflecting the mobilization of C from rock and fixation of N in aluminosilicate minerals at temperatures $> 80°C$. This finding builds on previous work demonstrating a link between N and potassium (K) in marine sediments [*Muller*, 1977] and in high-pressure metasedimentary rocks from subduction zones [*Bebout and Fogel*, 1992; *Busigny et al.*, 2003]. However, the relationship between N and K in metasedimentary rocks was significant though more variable when analyzed across all samples ($R^2 = 0.23$, $p < 0.001$, not shown) and when considering only high-pressure mica schist ($R^2 = 0.325$, $p < 0.001$, not shown). Such weaker correlation coefficients has been attributed to preferential N devolatilization (versus K) [*Busigny and Bebout*, 2013] at higher temperature regimes but may also reflect accumulation of detrital K-feldspars in the sediments [*Boyd*, 2001] or the presence of N in condensed organic phases protected by mineral association [*Boudou et al.*, 2008].

4.3. Spatial Distribution of Rock N Reservoirs

Differences in rock type and postdepositional processing give rise to substantial variation in rock N reservoirs at both local and regional scales. Segmenting our data by geomorphic province reveals substantial variation in the size of regional-scale N reservoirs (Figure 6), including numerous "hot regions" where median rock N contents exceed $2\,kg\,N\,m^{-3}$ (Figure 7c). These findings support the idea that N-rich rocks are widespread, with rock type abundance and geophysical constraints (i.e., depositional and thermal histories) serving as useful proxies for rock N contents.

Our model also points substantial N reservoirs in ecosystems dominated by both herbaceous and woody vegetation. Regionally, the distribution of rock N reservoirs was primarily associated with the distribution of dominant rock types (Figure 6). Median rock N reservoir estimates did not vary substantially between upland and alluvial landscapes, but upland ecosystems had a higher potential for large rock N reservoirs due to differences in density between alluvium versus the in situ bedrock. Desert in California hosted lower rock N reservoirs compared to grasslands and forests, primarily owing to the igneous lithologies and alluvial deposition regimes that dominated arid lands. More than a quarter of all forests and grasslands in the state

had rock N reservoirs in excess of 1 kg N m^{-3}, as these ecosystems were generally underlain by sedimentary lithologies of the California Coast Ranges.

At local scales, rock N reservoirs may be more variable than our model suggests, particularly in sites developing on sedimentary lithologies where depositional strata can vary at centimeter to meter scales. Among sampling sites where we observed multiple strata ($n = 119$, 22% of sampling sites), we analyzed three or more rock samples and found that the median range of observed N concentrations was 353 mg kg^{-1}, which could alter our rock N reservoir estimates by ~1 kg N m^{-3}. These findings suggest that assumptions of substrate homogeneity must be applied with caution when working at scales < ~1 m and that knowledge and sampling of the sedimentary stratigraphy is necessary to quantify rock N reservoirs, and their contribution to soil N pools at the scale of individual ecosystem stands.

4.4. Rock Nitrogen Denudation

Consistent with hypothesis two, tectonics and rock geochemistry more strongly regulated rock N denudation fluxes than lithology alone in our analysis. Nitrogen denudation rates were highest in regions with moderate-to-high relief (>500 m km^{-1}) and rock N concentrations > 500 mg kg^{-1}, and low among regions with low relief, irrespective of rock N content. At moderate-to-long time scales, the mobilization of N from rock sources to the terrestrial biosphere is controlled by interactions between rock N concentration and the rate of rock exhumation (i.e., physical plus chemical weathering). While the N denudation rate likely exceeds the rate of chemical N weathering in some ecosystems, chemical fluxes of elements generally scale with denudation fluxes [*Riebe et al.*, 2004]. Therefore, N denundation rates is a good predictor of the relative magnitude of the geologic N supply flux, except at very high denudation rates where chemical and denudation fluxes become decoupled due to climatic constraints on silicate-weathering kinetics [*Gabet and Mudd*, 2009; *West et al.*, 2005].

Our denudation model highlights the importance of synergistic interactions between lithology and tectonic uplift in determining N inputs to terrestrial ecosystems. In our model, 50% of the N denudation flux is derived from upland forest ecosystems (~30% of the land area), owing primarily to orographic controls on erosion, precipitation, and controls on the distribution of plant functional types across California. Given that water can be limiting in temperate and boreal biomes, these relationships suggest that rock N fluxes could contribute disproportionately to montane forests where orographic precipitation patterns, driven by mountainous topography, control the distribution of both vegetation types and erosion rates.

The role of climate in regulating rock N weathering is not explicitly considered in our model. Past studies have pointed to relatively poor correlations between climatic factors and denudation rates in the kinds of ecosystems we examined [*Riebe et al.*, 2001; *Portenga and Bierman*, 2011]. Biological availability and ecosystem utilization of the rock N sources is likely sensitive to climatic factors, but it is difficult to incorporate such controls into our model owing to uncertainties over the realized relationships between climate and weathering of silicate versus organic N reservoirs. Weathering of mineral N forms is probably climate dependent, as field analyses show that water availability strongly regulates acid hydrolysis kinetics at hillslope to basin scales [*Kump et al.*, 2000; *Riebe et al.*, 2004; *Rasmussen et al.*, 2011]. However, organic N reservoirs may not exhibit this same sensitivity, as oxidative weathering processes appear to be more dependent on rates of rock exhumation [*Bolton et al.*, 2006; *Calmels et al.*, 2007]. Further, weathering of rock N may not adhere to standard climate-dependent kinetic models, as biological demand for N may enhance the weathering of N-rich rocks via plant roots, mycorrhizal networks, and free-living microbes [*Jongmans et al.*, 1997]. A recent study by *Morford et al.*, 2016 showed that chemical depletion rates of N in sedimentary rocks exceeded those of other elements (K and Na) by ~20% across a range of temperate forest ecosystems. Future work addressing the interaction between organic and silicate N rock reservoirs, climate, and biology will greatly enhance the ability to project rock N inputs across terrestrial ecosystems [*Houlton and Morford*, 2015].

Our denudation model assumes that erosion rates scale with mean local relief; hence, the highest rates of N denudation are observed for the steepest terrains (Figure 7d). However, our analysis shows that high-relief areas (>1500 m km^{-1}) have only minor leverage on the total N denudation flux across California due to their limited areal extent (Figure 9b). Only 21% of the total N denudation flux originates from areas with relief greater than 1000 m km^{-1} and only 3% of the flux from areas with relief greater than 2000 m km^{-1}. Thus, while high-relief ecosystems exhibit the highest N denudation rates, landscapes with more moderate topography and N-rich lithology account for most of the total N denudation flux regionally (Figure 7).

There are limitations to statistical modeling approaches to denudation. In particular, grid-scale bias [*Zhang and Montgomery*, 1994] and selective sampling of high-relief landscapes [*Kirchner and Ferrier*, 2013] contribute to underestimation and overestimation of denudation fluxes in high-relief and low-relief landscapes, respectively. Furthermore, the application of ^{10}Be erosion rates may not accurately reflect denudation rates of fine-grained sedimentary rocks, as these lithologies do not contain quartz grains amenable to cosmogenic radionuclide geochemical analysis. Similar to biases derived from the regression model, these factors may contribute to an overestimation of N denudation among basins dominated by low-relief alluvial sediments or an underestimation of N denudation among high-relief areas with fine-grained sedimentary rocks, which can erode more rapidly due to lower rock strength than metamorphic or igneous rocks [*Aalto et al.*, 2006]. However, our model suggests that low-relief alluvial domains contribute only 13% of the total N denudation flux, thus pointing to a minimal effect of these possible limitations on our estimates overall.

In sum, our model is useful for segmenting spatial domains where rock N sources may contribute meaningfully to terrestrial N inputs across ecosystems. Geologic nitrogen is predominantly mobilized in regions with an abundance of sedimentary and metasedimentary rocks with moderate-to-high relief landscapes. While some exceptions exist owning to extreme relief (e.g., N-poor igneous lithologies of the southern Sierra Nevada escarpment and Mount Shasta), most ecosystems developing in igneous lithologies or areas of low relief have relatively low N denudation values, regardless of rock N reservoirs (Figures 7d and 8). Our spatial model points to numerous regional "hot spots" of high N denudation rates, including sedimentary and metasedimentary lithologies of the North Coast and Klamath Mountains, western Transverse Ranges, and the White Inyo Mountains of the Great Basin.

4.5. Implications of Rock N Reservoirs for Terrestrial N Supply

Our findings suggest that rock N comprises an important N input to forest and grassland ecosystems across California. Our model does not explicitly consider the chemical weathering component of the total denudation, which likely varies regionally owing to differences in climate and geobiological factors. However, local-scale investigations of chemical weathering of bedrock residuum in rapidly eroding headwater catchments of northwest California indicate that 37–47% of N is chemically released from silicate N reservoirs prior to transport [*Morford et al.*, 2016]. Erosion and redeposition of N-bearing minerals via colluvial and alluvial processes likely contributes to further chemical depletion of rock N reservoirs prior to export to the ocean. Further, organic N reservoirs weather more rapidly than silicates due to oxidative weathering [*Bolton et al.*, 2006; *Hilton et al.*, 2014; *Petsch et al.*, 2000]. Together, this suggests that chemical weathering comprises a substantial fraction of the total N denudation across California.

Our results suggest that rock N inputs could increase statewide N inputs to California ecosystems by 25–30%. Preindustrial (natural) atmospheric N inputs via deposition and fixation are estimated to be 140 $\pm$ 20 Gg N yr^{-1} statewide [*Dentener*, 2006; *Houlton et al.*, 2008]. Our model predicts N denudation fluxes on the order of 20–92 Gg yr^{-1} in California (median = 40 Gg N yr^{-1}). Even under conservative scenarios where N denudation is relatively low, inputs from rock are comparable to background N inputs via atmospheric deposition. Modern anthropogenic N inputs are thought to contribute ~ 150 Gg N yr^{-1} to California [*Liptzin et al.*, 2016], largely via the application of N fertilizers; but these N inputs are focused in agricultural lands and ecosystems downwind of urban sources (i.e., Central Valley and Los Angeles Basin). In contrast, high rock N input areas are concentrated among the mountain ranges adjacent to the Pacific Ocean and in northwestern California, where anthropogenic N inputs are relatively low [*National Atmospheric Deposition Program*, 2014].

Further, rock N reservoirs could contribute substantially to total soil N reservoirs, thus altering the mineralization of N to vegetation. Across the northern Coast Ranges, our model suggests that rock N reservoirs average 1–2 kg N m^{-3}. Assuming that soil is derived from 50 cm of bedrock, this rock N density could account for between 5 and 10 Mg ha^{-1} of soil N in the absence of N loss pathways (e.g., leaching and denitrification). In comparison, average total N storage in these soils ranges from 6.4 to 9.3 Mg ha^{-1} [*Post et al.*, 1985], suggesting that rock N contribution to soil N reservoirs may be similar, or larger, than atmospheric N inputs.

Local-scale empirical investigations in forests of northwestern California substantiate these predictions: 46–51% of total soil N is found in rock materials (4.8–7.0 Mg ha^{-1}), with rock accounting for as much as 80% of the total soil N [*Morford et al.*, 2016]. Given the size of this in situ reservoir, we suspect that rock N sources contribute to

Table 2. Estimates for Rock N Concentration (mg kg^{-1}) by Rock Type in This Study Versus Previous Compilations

	This Study	Li [1991]	Wedepohl [1995]	Holloway and Dahlgren [2002]	Kerrich et al. [2006]	Goldblatt et al. [2009]	Johansson et al. [2012]	Johnson and Goldblatt [2015]
Fine-grained sedimentary	698 (0–7152)	(600–1000)	-	(113–14000)	(73–9300)	700	(0–7900)[b]	860
Coarse-grained sedimentary	271 (57–3680)	-	-	(17–1947)	-	250		230
Carbonates	300 (45–1910)	-	-	(20–7000)	-	100	(23–2400)	130
Siliceous	157 (53–1792)	-	-	(0–100)	-	-	(62–1997)	-
Igneous	80 (0–280)	-	60[c]	(0–250)	-	35	-	5 - 52
Metamorphic (high grade)	148 (41–358)	-	-	(13–422)	(20–800)	250	-	200

[a]Average values are presented where they are available, and value ranges are presented in parenthesis. Fine-grained sedimentary includes mudstone, shale, argillite, slate, phyllite, and mica schist. Coarse-grained sedimentary includes conglomerate, sandstone, graywacke, and quartzite. Estimates from the SedDB [Johansson et al., 2012] are reported only for values from > 100 m below sea floor.
[b]SedDB estimates for bulk siliciclastic deposits (i.e., in coarse- and fine-grained sediments combined, median value was 900 mg kg^{-1}).
[c]Represents average value of upper continental crust, including 14% sedimentary rocks by mass.

the development of ecosystem nutrient pools in a way that mimics other important rock-derived nutrients such as calcium and phosphorus [Walker and Syers, 1976].

The rock N denudation flux presented here does not consider incomplete chemical weathering of regolith beneath the plant-rooting zone. Unweathered sedimentary organic matter can be directly transferred to the marine environment from small mountainous watersheds at active tectonic margins [Blair et al., 2003], suggesting that the residence time of rock N in the weathering zone is an important factor in controlling rock N supplies. In contrast, if chemical weathering of rock N occurs at depth within soils and regolith, some or all of the N may be released to groundwater, transported to fluvial systems, or denitrified, thus bypassing land ecosystems [Hendry et al., 1984; Holloway et al., 1998; Strathouse et al., 1980]. The ability of terrestrial plant communities to utilize this deeply weathered N is dependent on the depth to which the critical zone penetrates into the subsurface environment.

4.6. Global Distribution of Rock N Reservoirs

Our analysis builds on previous compilations of N concentrations in rocks and sediments [Holloway and Dahlgren, 2002; Johansson et al., 2012; Kerrich et al., 2006; Johnson and Goldblatt, 2015], and N abundance estimates among geologic reservoirs [Goldblatt et al., 2009; Li, 1991; Wedepohl, 1995] (Table 2). Together, our results combined with past data argue for a large and extensive reservoir of reactive N in the Earth system. Sedimentary and metasedimentary rocks occupy ~ 70% of the Earth surface [Durr et al., 2005], with fine-grained rocks comprising ~ 40% of these reservoirs [Suchet et al., 2003]. While the global weathering flux of rock N remains uncertain, N burial in marine sediments [Gruber and Galloway, 2008] substantially exceeds the volcanic degassing flux and transfer to the mantle [Vincent Busigny et al., 2011; Sano et al., 2001], suggesting that a large weathering flux of rock N (~15–25 Tg N yr^{-1}) is required to balance ocean burial of N at geologic time scales [Berner, 2006; Boyd, 2001].

References

Aalto, R., T. Dunne, and J. L. Guyot (2006), Geomorphic controls on Andean denudation rates, J. Geol., 114(1), 85–99.
Balco, G., N. Finnegan, A. Gendaszek, J. O. H. Stone, and N. Thompson (2013), Erosional response to northward-propagation crustal thickening in the Coastal Ranges of the U.S. Pacific Northwest, Am. J. Sci., 313(8), 790–806.
Beaudette, D. E., P. Roudier, and A. T. O'Geen (2013), Algorithms for quantitative pedology: A toolkit for soil scientists, Comput. Geosci., 52, 258–268.
Bebout, G. E., and M. L. Fogel (1992), Nitrogen-isotope compositions of metasedimentary rocks in the Catalina Schist, California: Implications for metamorphic devolatilization history, Geochim. Cosmochim. Acta, 56(7), 2839–2849.
Bebout, G. E., D. C. Cooper, A. D. Bradley, and S. J. Sadofsky (1999), Nitrogen-isotope record of fluid-rock interactions in the Skiddaw Aureole and granite, English Lake District, Am. Mineral., 84(10), 1495–1505.
Berner, R. A. (2006), Geological nitrogen cycle and atmospheric N-2 over Phanerozoic time, Geology, 34(5), 413–415.
Blair, N. E., E. L. Leithold, S. T. Ford, K. A. Peeler, J. C. Holmes, and D. W. Perkey (2003), The persistence of memory: The fate of ancient sedimentary organic carbon in a modern sedimentary system, Geochim. Cosmochim. Acta, 67(1), 63–73.

Bolton, E. W., R. A. Berner, and S. T. Petsch (2006), The weathering of sedimentary organic matter as a control on atmospheric O-2: II. Theoretical modeling, *Am. J. Sci.*, *306*(8), 575–615.

Boudou, J. P., A. Schimmelmann, M. Ader, M. Mastalerz, M. Sebilo, and L. Gengembre (2008), Organic nitrogen chemistry during low-grade metamorphism, *Geochim. Cosmochim. Acta*, *72*(4), 1199–1221.

Boyd, S. R. (2001), Nitrogen in future biosphere studies, *Chem. Geol.*, *176*(1–4), 1–30.

Busigny, V., and G. E. Bebout (2013), Nitrogen in the silicate Earth: Speciation and isotopic behavior during mineral-fluid interactions, *Elements*, *9*(5), 353–358.

Busigny, V., P. Cartigny, P. Philippot, M. Ader, and M. Javoy (2003), Massive recycling of nitrogen and other fluid-mobile elements (K, Rb, Cs, H) in a cold slab environment: Evidence from HP to UHP oceanic metasediments of the Schistes Lustres nappe (western Alps, Europe), *Earth Planet. Sci. Lett.*, *215*(1–2), 27–42.

Busigny, V., P. Cartigny, and P. Philippot (2011), Nitrogen isotopes in ophiolitic metagabbros: A re-evaluation of modern nitrogen fluxes in subduction zones and implication for the early Earth atmosphere, *Geochim. Cosmochim. Acta*, *75*(23), 7502–7521.

California Geological Survey (2002), California geomorphic provinces, note 36, Based on the Geomorphic Map of California prepared by Olaf P. Jennings, 1938. Revisions of the text by D.L. Wagner, 2002.

Calmels, D., J. Gaillardet, A. Brenot, and C. France-Lanord (2007), Sustained sulfide oxidation by physical erosion processes in the Mackenzie River basin: Climatic perspectives, *Geology*, *35*(11), 1003–1006.

Ciais, P., et al. (2013), Carbon and other biogeochemical cycles, in *Climate Change 2013: The Physical Science Basis. Contribution of Working Group I to the Fifth Assessment Report of the Intergovernmental Panel on Climate Change*, edited by T. F. Stocker et al., Cambridge Univ. Press, Cambridge, U. K., and New York.

Cleveland, C. C., B. Z. Houlton, W. K. Smith, A. R. Marklein, S. C. Reed, W. Parton, S. J. Del Grosso, and S. W. Running (2013), Patterns of new versus recycled primary production in the terrestrial biosphere, *Proc. Natl. Acad. Sci. U.S.A.*, *110*(31), 12,733–12,737.

Compton, J. S., L. B. Williams, and R. E. Ferrell (1992), Mineralization of organogenic ammonium in the Monterey Formation, Santa-Maria basin and San-Joaquin basin, California, USA, *Geochim. Cosmochim. Acta*, *56*(5), 1979–1991.

Cornwell, S. M., and E. L. Stone (1968), Availability of nitrogen to plants in acid coal mine spoils, *Nature*, *217*(5130), 768–769.

Dentener, F. J. (2006), *Global Maps of Atmospheric Nitrogen Deposition, 1860, 1993, and 2050, Data Set*, Oak Ridge Natl. Lab., Distributed Active Archive Center, Oak Ridge, Tenn.

Dixon, J. C., S. W. Campbell, and B. Durham (2012), Geologic nitrogen and climate change in the geochemical budget of Karkevagge, Swedish Lapland, *Geomorphology*, *167*, 70–76.

Durr, H. H., M. Meybeck, and S. H. Durr (2005), Lithologic composition of the Earth's continental surfaces derived from a new digital map emphasizing riverine material transfer, *Global Biogeochem. Cycles*, *19*, GB4S10, doi:10.1029/2005GB002515.

Gabet, E. J., and S. M. Mudd (2009), A theoretical model coupling chemical weathering rates with denudation rates, *Geology*, *37*(2), 151–154.

Gaillardet, J., B. Dupre, P. Louvat, and C. J. Allegre (1999), Global silicate weathering and CO_2 consumption rates deduced from the chemistry of large rivers, *Chem. Geol.*, *159*(1–4), 3–30.

Goldblatt, C., M. W. Claire, T. M. Lenton, A. J. Matthews, A. J. Watson, and K. J. Zahnle (2009), Nitrogen-enhanced greenhouse warming on early Earth, *Nat. Geosci.*, *2*(12), 891–896.

GRASS Development Team (2012), Geographic Resources Analysis Support System (GRASS GIS) software.

Gruber, N., and J. N. Galloway (2008), An Earth-system perspective of the global nitrogen cycle, *Nature*, *451*(7176), 293–296.

Gudmundsdottir, M. H., K. Blisniuk, Y. Ebert, N. M. Levine, D. H. Rood, A. Wilson, and G. E. Hilley (2013), Restraining bend tectonics in the Santa Cruz Mountains, California, imaged using Be-10 concentrations in river sands, *Geology*, *41*(8), 843–846.

Hartnett, H. E., R. G. Keil, J. I. Hedges, and A. H. Devol (1998), Influence of oxygen exposure time on organic carbon preservation in continental margin sediments, *Nature*, *391*(6667), 572–575.

Hedges, J. I., and R. G. Keil (1995), Sedimentary organic-matter preservation: An assessment and speculative synthesis, *Mar. Chem.*, *49*(2–3), 81–115.

Hendry, M. J., R. G. L. McCready, and W. D. Gould (1984), Distribution, source and evolution of nitrate in a glacial till of southern Alberta, Canada, *J. Hydrol.*, *70*(1–4), 177–198.

Hilton, R. G., J. Gaillardet, D. Calmels, and J. L. Birck (2014), Geological respiration of a mountain belt revealed by the trace element rhenium, *Earth Planet. Sci. Lett.*, *403*, 27–36.

Hoefs, J. (2009), *Stable Isotope Geochemistry*, 6th ed., Springer, Berlin.

Holloway, J. M., and R. A. Dahlgren (2002), Nitrogen in rock: Occurrences and biogeochemical implications, *Global Biogeochem. Cycles*, *16*(4), 1118, doi:10.1029/2002GB001862.

Holloway, J. M., R. A. Dahlgren, B. Hansen, and W. H. Casey (1998), Contribution of bedrock nitrogen to high nitrate concentrations in stream water, *Nature*, *395*(6704), 785–788.

Houlton, B. Z., and S. L. Morford (2015), A new synthesis for terrestrial nitrogen inputs, *Soil*, *1*(1), 381–397.

Houlton, B. Z., Y.-P. Wang, P. M. Vitousek, and C. B. Field (2008), A unifying framework for dinitrogen fixation in the terrestrial biosphere, *Nature*, *454*(7202), 327–330.

Howard, A. D., W. E. Dietrich, and M. A. Seidl (1994), Modeling fluvial erosion on regional to continental scales, *J. Geophys. Res.*, *99*(B7), 13,971–13,986, doi:10.1029/94JB00744.

Hungate, B. A., J. S. Dukes, M. R. Shaw, Y. Q. Luo, and C. B. Field (2003), Nitrogen and climate change, *Science*, *302*(5650), 1512–1513.

Hutchinson, G. E. (1944), Nitrogen in the biogeochemistry of the atmosphere, *Am. Sci.*, *32*(3), 178–195.

Javoy, M., and F. Pineau (1991), The volatiles record of a popping rock from the mid-Atlantic ridge at 14-degrees-N: Chemical and isotopic composition of gas trapped in the vesicles, *Earth Planet. Sci. Lett.*, *107*(3–4), 598–611.

Johansson, A., K. Lehnert, and L. Hsu (2012), Status report on the SedDB sediment geochemistry database, *GeoPRISMS Newsletter*, p. 21.

Johnson, B., and C. Goldblatt (2015), The nitrogen budget of Earth, *Earth Sci. Rev.*, *148*, 150–173.

Jongmans, A. G., N. van Breemen, U. Lundstrom, P. A. W. vanHees, R. D. Finlay, M. Srinivasan, T. Unestam, R. Giesler, P. A. Melkerud, and M. Olsson (1997), Rock-eating fungi, *Nature*, *389*(6652), 682–683.

Jurisch, S. A., S. Heim, B. M. Krooss, and R. Littke (2012), Systematics of pyrolytic gas (N-2, CH_4) liberation from sedimentary rocks: Contribution of organic and inorganic rock constituents, *Int. J. Coal Geol.*, *89*(1), 95–107.

Kennedy, M. J., D. R. Pevear, and R. J. Hill (2002), Mineral surface control of organic carbon in black shale, *Science*, *295*(5555), 657–660.

Kerrich, R., Y. Jia, C. Manikyamba, and S. M. Naqvi (2006), Secular variations of N-isotopes in terrestrial reservoirs and ore deposits, *Geol. Soc. Am. Mem.*, *198*, 81–104.

Kirchner, J. W., and K. L. Ferrier (2013), Earth science: Mainly in the plain, *Nature*, *495*(7441), 318–319.

Koenker, R. (2013), quantreg: Quantile regresion. R package version 5.05. [Available at http://CRAN.R-project.org/package=quantreg.]

Koenker, R., and J. A. Machado (1999), Goodness of fit and related inference processes for quantile regression, *J. Am. Stat. Assoc.*, *94*(448), 1296–1310.

Kump, L. R., S. L. Brantley, and M. A. Arthur (2000), Chemical, weathering, atmospheric CO_2, and climate, *Annu. Rev. Earth Planet. Sci., 28*, 611–667.

Li, Y. H. (1991), Distribution patterns of the elements in the ocean: A synthesis, *Geochim. Cosmochim. Acta, 55*(11), 3223–3240.

Liptzin, D., R. A. Dahlgren, and T. Harter (2016), Chapter 4: A California nitrogen mass balance for 2005, in *The California Nitrogen Assessment: Challenges and Solutions for People, Agriculture, and the Environment*, edited by T. P. Tomich et al., Univ. of California Press, Oakland, Calif.

Ludington, S., B. C. Moring, R. J. Miller, K. S. Flynn, and M. J. Hopkins (2005), Open-file report OF-2005-1305: Preliminary integrated databases for the United States—Western States: California, Nevada, Arizona, and Washington, U.S. Geol. Surv., Reston, Va.

Maher, K., and C. P. Chamberlain (2014), Hydrologic regulation of chemical weathering and the geologic carbon cycle, *Science, 343*(6178), 1502–1504.

Marty, B. (1995), Nitrogen-content of the mantle inferred from N-2-Ar correlation in oceanic basalts, *Nature, 377*(6547), 326–329.

Miller, N. H. J. (1903), The amounts of nitrogen and organic carbon in some clays and marls, *Q. J. Geol. Soc., 59*, 133–141.

Montgomery, D. R., and M. T. Brandon (2002), Topographic controls on erosion rates in tectonically active mountain ranges, *Earth Planet. Sci. Lett., 201*(3–4), 481–489.

Montross, G. G., B. L. McGlynn, S. N. Montross, and K. K. Gardner (2013), Nitrogen production from geochemical weathering of rocks in southwest Montana, USA, *J. Geophys. Res. Biogeosci., 118*, 1068–1078, doi:10.1002/jgrg.20085.

Morford, S. L., B. Z. Houlton, and R. A. Dahlgren (2011), Increased forest ecosystem carbon and nitrogen storage from nitrogen rich bedrock, *Nature, 477*(7362), 78–81.

Morford, S. L., B. Z. Houlton, and R. A. Dahlgren (2016), Direct quantification of long-term rock nitrogen inputs to temperate forest ecosystems, *Ecology, 97*(1), doi:10.1890/15-0501.1.

Muller, P. J. (1977), C-N ratios in Pacific deep-sea sediments: Effect of inorganic ammonium and organic nitrogen-compounds sorbed by clays, *Geochim. Cosmochim. Acta, 41*(6), 765–776.

National Atmospheric Deposition Program (2014), National Atmospheric Deposition Program 2013 Annual Summary, NADP Data Report 2014-01, Illinois State Water Survey, Univ. of Illinois at Urbana-Champaign, Ill.

Petsch, S. T., R. A. Berner, and T. I. Eglinton (2000), A field study of the chemical weathering of ancient sedimentary organic matter, *Org. Geochem., 31*(5), 475–487.

Pitcairn, I. K., D. A. H. Teagle, R. Kerrich, D. Craw, and T. S. Brewer (2005), The behavior of nitrogen and nitrogen isotopes during metamorphism and mineralization: Evidence from the Otago and Alpine Schists, New Zealand, *Earth Planet. Sci. Lett., 233*(1–2), 229–246.

Portenga, E. W., and P. R. Bierman (2011), Understanding Earth's eroding surface with [10]Be, *GSA Today, 21*(8), 4–10.

Post, W. M., J. Pastor, P. J. Zinke, and A. G. Stangenberger (1985), Global patterns of soil-nitrogen storage, *Nature, 317*(6038), 613–616.

R Core Team (2014), *R: A Language and Environment for Statistical Computing*, R Foundation for Statistical Computing, Vienna, Austria.

Rasmussen, C., S. Brantley, D. D. Richter, A. Blum, J. Dixon, and A. F. White (2011), Strong climate and tectonic control on plagioclase weathering in granitic terrain, *Earth Planet. Sci. Lett., 301*(3–4), 521–530.

Rayleigh, L. (1939), Nitrogen, argon and neon in the Earth's crust with applications to cosmology, *Proc. R. Soc. Lond. A Math. Phys. Sci., 170*(943), 451–464.

Riebe, C. S., J. W. Kirchner, D. E. Granger, and R. C. Finkel (2001), Minimal climatic control on erosion rates in the Sierra Nevada, California, *Geology, 29*(5), 447–450.

Riebe, C. S., J. W. Kirchner, and R. C. Finkel (2004), Erosional and climatic effects on long-term chemical weathering rates in granitic landscapes spanning diverse climate regimes, *Earth Planet. Sci. Lett., 224*(3–4), 547–562.

Sadofsky, S. J., and G. E. Bebout (2003), Record of forearc devolatilization in low-T, high-P/T metasedimentary suites: Significance for models of convergent margin chemical cycling, *Geochem. Geophys. Geosyst., 4*(4), 9003, doi:10.1029/2002GC000412.

Sano, Y., N. Takahata, Y. Nishio, T. P. Fischer, and S. N. Williams (2001), Volcanic flux of nitrogen from the Earth, *Chem. Geol., 171*(3–4), 263–271.

Silva, J. A., and J. M. Bremner (1966), Determination and isotope-ratio analysis of different forms of nitrogen in soils. 5. Fixed ammonium, *Soil Sci. Soc. Am. Proc., 30*(5), 587–594.

Stallard, R. F., and J. M. Edmond (1983), Geochemistry of the Amazon 2. The influence of geology and weathering environment on the dissolved-load, *J. Geophys. Res., 88*, 9671–9688, doi:10.1029/JC088iC14p09671.

Stevenson, F. J. (1959), Presence of fixed ammonium in rocks, *Science, 130*(3369), 221–222.

Strathouse, S. M., G. Sposito, P. J. Sullivan, and L. J. Lund (1980), Geologic nitrogen: A potential geochemical hazard in the San-Joaquin Valley, California, *J. Environ. Qual., 9*(1), 54–60.

Suchet, P. A., J. L. Probst, and W. Ludwig (2003), Worldwide distribution of continental rock lithology: Implications for the atmospheric/soil CO_2 uptake by continental weathering and alkalinity river transport to the oceans, *Global Biogeochem. Cycles, 17*(2), 1038, doi:10.1029/2002GB001891.

Summerfield, M. A., and N. J. Hulton (1994), Natural controls of fluvial denudation rates in major world drainage basins, *J. Geophys. Res., 99*(B7), 13,871–13,883, doi:10.1029/94JB00715.

U.S. Geological Survey (2004), *Shuttle Radar Topography Mission*, Global Land Cover Facility,Univ. of Maryland, College Park, Md.

Vitousek, P. M., and R. W. Howarth (1991), Nitrogen limitation on land and in the sea: How can it occur, *Biogeochemistry, 13*(2), 87–115.

Walker, T. W., and J. K. Syers (1976), Fate of phosphorus during pedogenesis, *Geoderma, 15*(1), 1–19.

Wang, Y. P., and B. Z. Houlton (2009), Nitrogen constraints on terrestrial carbon uptake: Implications for the global carbon-climate feedback, *Geophys. Res. Lett., 36*, L24403, doi:10.1029/2009GL041009.

Wedepohl, K. H. (1995), The composition of the continental crust, *Geochim. Cosmochim. Acta, 59*(7), 1217–1232.

West, A. J., A. Galy, and M. Bickle (2005), Tectonic and climatic controls on silicate weathering, *Earth Planet. Sci. Lett., 235*(1–2), 211–228.

Willenbring, J. K., A. T. Codilean, and B. McElroy (2013), Earth is (mostly) flat: Apportionment of the flux of continental sediment over millennial time scales, *Geology, 41*(3), 343–346.

Williams, L. B., and R. E. Ferrell (1991), Ammonium substitution in illite during maturation of organic-matter, *Clays Clay Miner., 39*(4), 400–408.

Williams, L. B., B. R. Wilcoxon, R. E. Ferrell, and R. Sassen (1992), Diagenesis of ammonium during hydrocarbon maturation and migration, Wilcox-Group, Louisiana, *Appl. Geochem., 7*(2), 123–134.

Zhang, W. H., and D. R. Montgomery (1994), Digital elevation model grid size, landscape representation, and hydrologic simulations, *Water Resour. Res., 30*(4), 1019–1028, doi:10.1029/93WR03553.